Spin Hall magnetoresistance in the non-collinear ferrimagnet GdIG close to the compensation temperature

Bo-Wen Dong,[1,2,3] Joel Cramer,[2,3] Kathrin Ganzhorn,[4,5] H. Y. Yuan,[3,6] Er-Jia Guo,[3,7] Sebastian T. B. Goennenwein,[4,5,8,9] and Mathias Kläui[2,3]

[1]*School of Materials Science and Engineering, University of Science and Technology Beijing, 100083 Beijing, China*
[2]*Graduate School of Excellence Materials Science in Mainz (MAINZ), 55128 Mainz, Germany*
[3]*Institute of Physics, Johannes Gutenberg-Universität Mainz, 55099 Mainz, Germany*
[4]*Walther-Meißner-Institut, Bayerische Akademie der Wissenschaften, 85748 Garching, Germany*
[5]*Physik-Department, Technische Universität München, 85748 Garching, Germany*
[6]*Department of Physics, Southern University of Science and Technology, Shenzhen, 518055 Guangdong, China*
[7]*Quantum Condensed Mater Division, Oak Ridge National Laboratory, Oak Ridge, Tennessee 37830, USA*
[8]*Institut für Festkörper- und Materialphysik, Technische Universität Dresden, 01062 Dresden*
[9]*Center for Transport and Devices of Emergent Materials, Technische Universität Dresden, 01062 Dresden*

Abstract:

We investigate the spin Hall magnetoresistance (SMR) in a gadolinium iron garnet (GdIG)/platinum (Pt) heterostructure by angular dependent magnetoresistance measurements. The magnetic structure of the ferromagnetic insulator GdIG is non-collinear near the compensation temperature, while it is collinear far from the compensation temperature. In the collinear regime, the SMR signal in GdIG is consistent with the usual $\sin^2\theta$ relation well established in the collinear magnet yttrium iron garnet (YIG), with θ the angle between magnetization and spin Hall spin polarization direction. In the non-collinear regime, both a SMR signal with inverted sign and a more complex angular dependence with four maxima are observed within one sweep cycle. The number of maxima as well as the relative strength of different maxima depend strongly on temperature and field strength. Our results evidence a complex SMR behavior in the non-collinear magnetic regime that goes beyond the conventional formalism developed for collinear magnetic structures.

1. Introduction

Emerging phenomena driven by spin currents have attracted much attention in recent years due to their potential to circumvent Oersted fields and reduce Joule heating in spintronic devices [1,2]. In ferromagnetic insulators (FMI), pure spin currents can be generated for instance by spin pumping [2-6] or the spin Seebeck effect (SSE) [7-16]. The conversion of charge currents to spin currents via spin-orbit coupling in non-magnetic metals is referred to as the spin Hall effect (SHE) [17-19], while the inverse process is the inverse spin Hall effect (ISHE) [20,21]. In FMI/heavy metal (HM) systems, spin currents with a polarization $\boldsymbol{\sigma}$ generated by the SHE in the HM flow towards the FMI/HM interface and are either reflected ($\boldsymbol{\sigma} \parallel \boldsymbol{M}$) by the interface or absorbed by the magnetization $\boldsymbol{M}$ of FMI due to spin-transfer torque ($\boldsymbol{\sigma} \perp \boldsymbol{M}$) [22]. The reflected transverse spin currents are re-converted into a longitudinal charge current by the ISHE, adding to the originally applied current. Thus, the simultaneous action of SHE and ISHE in the HM leads to a dependence of the HM resistivity on the magnetization orientation of the adjacent FMI, giving rise to the spin Hall magnetoresistance (SMR) [23-26]. In the widely accepted SMR picture, the measured resistivity of the HM is given by $\rho = \rho_0 + \Delta\rho(\boldsymbol{M} \cdot \boldsymbol{\sigma})^2$, where ρ_0 is the

magnetization independent electric resistivity of the HM and $\Delta\rho$>0 is the change of resistivity due to the SMR [9,23-25]. In conventional collinear magnetic structures, the SMR thus is described by a $\sin^2\theta$ angular dependence when rotating $\boldsymbol{M}$ by a magnetic field $\boldsymbol{H}$ in the sample plane with θ the angle between $\boldsymbol{M}$ and $\boldsymbol{\sigma}$.

So far, most SMR studies focus on ferrimagnetic materials with collinear magnetic sublattices [23,27-31], while there are only a few studies for non-collinear magnetic systems [32-34]. The best known magnetic garnet material, yttrium iron garnet ($Y_3Fe_5O_{12}$, YIG), has been widely used in the study of the SMR due to its large insulating band gap (2.85 eV) [35] and magnetic softness, which allows for the accurate control of magnetization via relatively small magnetic fields. To form a non-collinear magnetization state in YIG, magnetic fields of a few hundred Tesla are required to induce the spin-flop transition [36], which is difficult to realize in practice. An alternative way to introduce a non-collinear magnetization is to replace the non-magnetic Y^{3+} ions in YIG by magnetic rare-earth ions such as Gd^{3+}. The resulting magnetic structure of gadolinium iron garnet ($Gd_3Fe_5O_{12}$, GdIG) comprises three magnetic sublattices, including a-site Fe^{3+} atoms octahedrally coordinated by O^{2-} ions, d-site Fe^{3+} atoms tetrahedrally coordinated by O^{2-} ions and c-site Gd^{3+} atoms dodecahedrally coordinated by O^{2-} ions. The moments of a-site Fe^{3+} are antiferromagnetically coupled to those of d-site Fe^{3+} and exhibit weak ferromagnetic coupling to the moments of c-site Gd^{3+}. The magnetization of the Gd^{3+} sublattice is very sensitive to temperature and the magnetic moments of the three sublattices cancel each other at the compensation temperature (T_{comp}), where the net spontaneous magnetization of GdIG vanishes. A non-collinear magnetization state can be achieved by applying a field of several Tesla around T_{comp}. Previously, GdIG has been used to study the SSE, in which a distinct sign change of the SSE signal is observed around T_{comp} [14] and in (In,Y)co-doped GdIG an inversion of the SMR signal was observed close to T_{comp} [33]. However it is unclear if this is a universal behavior and this surprising observation calls for studying this phenomenon in other compensated ferrimagnets in more detail.

In this manuscript, we investigate the effects of non-collinear magnetization of the prototypical three sublattice ferrimagnet GdIG and study the resulting SMR near its compensation point T_{comp}. We determine the angular dependent magnetoresistance (ADMR) – the evolution of ρ with H orientation -- around this temperature and find four maxima instead of the typical 2 maxima characteristic of the $\sin^2\theta$ angular dependence observed in the collinear regime. We ascertain the relative strength of these maxima as a function of temperature as well as magnetic field to determine the behavior of the SMR in this regime based on the configurations of the sublattice magnetizations.

2. Experimental

GdIG thin films with 100 nm thickness are grown by pulsed laser deposition (PLD) on commercial (100) oriented gadolinium gallium garnet ($Gd_3Ga_5O_{12}$, GGG) substrates and 5.5 nm of Pt is deposited *ex-situ* by magnetron sputtering [14]. Pt is commonly used in SMR studies due to its large spin Hall angle [19]. Two Pt stripes, each with a width of 100 μm and a length of 4 mm, separated by 1 mm, were patterned by optical lithography and subsequent ion milling. The measurement scheme of our GdIG/Pt sample is shown in Fig. 1(a) and the applied charge current *I* is aligned along the x axis in all our transport measurements. Figure 1(b) shows temperature dependent magnetization measurements of a GdIG sample recorded at a magnetic field of 0.1 T by superconducting quantum interference (SQUID) magnetometry. The magnetization first decreases with decreasing temperature before eventually increasing again. T_{comp} is observed around 180 K, which is lower than the bulk value of 288 K [37]. This is probably the result of strain effects in the film on the GGG substrate [38]. Due to the lower T_{comp}, it is relatively easy to study the SMR across a wide temperature range that comprises both collinear and non-collinear magnetization regimes of GdIG by using a cryostat with a variable temperature insert (10 K ~ 300 K).

3. Results and Discussion

We first rotate $\boldsymbol{M}$ via a magnetic field of 0.8 T in the xy, xz, and yz planes at 295 K in the collinear magnetization regime (see Fig. 1(a)) and measure the corresponding resistivity. The results are shown as red, blue and pink curves in Fig. 1(c), respectively. As the spin current polarization $\boldsymbol{\sigma}$ points along the y axis at the FMI/NM interface, the small variation of the resistance $\boldsymbol{R}$ when rotating $\boldsymbol{M}$ in the xz plane, where θ keeps a constant value of 90°, indicates that magnetic proximity induced anisotropic magnetoresistance (AMR) effects are negligible.[39] When rotating $\boldsymbol{M}$ within the yz plane, the ADMR shows a clear $\sin^2\beta$ angular dependence, which is a direct evidence for the SMR and also indicates a collinear magnetization that is aligned with the applied field direction ($\theta = \beta$). For the xy scan the MR is also dominated by the SMR and the inverted SMR signal is due to $\theta = 90° - \alpha$.

Secondly, we extract the SMR ratio of the GdIG/Pt sample from ADMR measurements in the yz plane as a function of temperature at a magnetic field of 0.8 T. The SMR ratio, defined as

$$\text{SMR ratio} = \frac{R(\beta=90°)-R(\beta=0°)}{R(\beta=0°)} \quad (1)$$

is plotted as red open circles in Fig. 2. As the temperature decreases from room temperature to 10 K, the SMR ratio shows a non-monotonic temperature dependence and reveals a minimum near $T_{\mathrm{comp}} \approx 180$ K.

For comparison, we also measure the temperature dependent SMR ratio in the same thickness Pt (5.5 nm) film deposited in nominally the same conditions onto a YIG slab also using the same experimental configuration for the measurements. Shown as blue open squares in Fig. 2, no dip of the SMR ratio is observed for YIG/Pt. The value of the SMR ratio in GdIG/Pt is similar to that in YIG/Pt at temperatures above 200 K and below 160 K, which corresponds to the collinear magnetic phase of GdIG [33] (see upper part of Fig. 2) and the SMR follows $\sin^2\beta$ angular dependence (see the insert of Fig. 2). As YIG keeps its collinear magnetic structure unchanged across the whole temperature range and GdIG exhibits a non-collinear canted magnetization near the compensation temperature, the drastic change of SMR ratio with temperature could be a result of the canted magnetization of GdIG in this temperature and field range. Note that the SMR ratios in the 2 samples show both similar temperature dependence and amplitude at temperatures far from T_{comp} (the collinear regime of GdIG). GdIG and YIG both belong to the material family of magnetic garnets, and therefore share the same crystal structure as described above. Given that the apart from the different garnet materials the other conditions are nominally identical and, we attribute the similar amplitude of SMR ratios in the YIG and GdIG based samples to similar interface conditions, e.g. a similar spin mixing conductance and a similar behavior of both garnets. This indicates that the Fe ions in both GdIG and YIG potentially dominate the spin transfer to the Pt as the Fe^{3+} density is similar in both garnets, while the Gd^{3+} moments (and obviously the non-magnetic Y^{3+}) play a much smaller role for the SMR. Similar conclusions were drawn in previous SMR measurements in (In, Y) doped GdIG [33]. Given the fact that the 4f orbital of Gd^{3+} is half-filled, which results in a zero-orbital angular momentum unlike in the case of Fe^{3+}, this observation could also indicates a potential impact of the orbital angular momentum on the spin mixing conductance.

To further investigate the SMR signal around T_{comp}, we measure the change of resistance ($\Delta R = R(\beta) - R(\beta = 0°)$) with the rotation angle of the fixed magnetic field 0.8 T in the yz plane for temperatures ranging from 183 K to 175 K in detail as shown in Fig. 3. Visible in the inset of Fig. 2, at T = 210 K, a typical $\sin^2\beta$ dependence is observed with maxima for $\beta = 90°$ and $270°$. When the temperature decreases to 183 K (Fig. 3(a)), the ΔR curve drops abruptly near $\beta = 180°$ and $360°$, while the curve exhibits broad maxima around $\beta = 90°$ and $270°$. At T = 181 K (Fig. 3(b)), ΔR decreases and two local minima appear around the out-of-plane field orientation ($\beta = 90°$ and $270°$), where two wide maxima were observed at 183 K. By further decreasing the temperature to 180 K (Fig. 3(c)), which is very close to T_{comp}, a SMR signal with inverted sign is observed. This SMR sign

inversion arises from the canted magnetic moments in GdIG. For instance, the sublattice moments of a-site Fe^{3+} and d-site Fe^{3+} are antiparallel to each other owing to the strong exchange coupling, but both are aligned perpendicularly to the external magnetic field in the canted phase, resulting in a sign change in the SMR. The inverted SMR due to non-collinear magnetic structures have also been observed in the InYGdIG/Pt heterostructure [33].

At T = 179 K (Fig. 3(d)), fine maxima appear around $\beta = 90°$ and $270°$, while the main maxima around $\beta = 180°$ and $360°$ remain. As the temperature is reduced further (Fig. 3(e) and Fig. 3(f)), the fine maxima grow and become comparable with the main maxima at $180°$ and $360°$ near T = 175 K. Finally, when the temperature reaches 160 K (inset of Fig. 2), the original $\sin^2\beta$ dependence observed for $T \gg T_{\mathrm{comp}}$ is recovered. To gain further insight into the origin of these multiple maxima not present in the collinear regime, we simultaneously measure the angular dependent SMR of two different parallel Pt stripes on one GdIG sample. The resistance changes of the two stripes are virtually identical under the rotating field (Fig. S1(a) and (b) in the supplemental material) confirming that on the size-scale of the contacts the sample shows a similar behaviour everywhere. Furthermore, we performed field rotation measurements in opposite directions, i.e. first clockwise (from 0° to 360°) then counterclockwise (from 360° back to 0°), shown in Fig. S1(c) and (d) in the supplemental material. The clear hysteresis behavior of the resistance maximum around β = 180°, suggests the existence of multi-domain states under 0.8 T external magnetic field. A possible explanation can be based on the assumption that some of the domains have a collinear magnetic structure, where $\boldsymbol{M}$ is parallel to the applied field, such that these domains contribute a SMR signal with maxima around $\beta = 90°$ and $270°$. On the other hand, the remaining domains feature a non-collinear magnetic structure with canted $\boldsymbol{M}$, which leads to the "inverted" SMR maxima around $\beta = 180°$ and $360°$. While an unambiguous determination of the spin structure from the observed SMR angular dependence is not straightforwardly possible, we can qualitatively model the SMR behavior by assuming different domain configurations and calculating the corresponding SMR response (see part II of the supplemental materials). The solid black lines in Fig. 3 represent the simulated SMR response derived from this approach and fit the experimental data well for 183 K and 181 K. We can thus attribute the more complex multi-maxima behavior to the formation of magnetic domains with different magnetic sublattice configurations in the GdIG. In particular, the relative abundance of domains with collinear sublattice magnetizations and of domains with non-collinear, canted sublattice magnetizations could change as a function of H and T, due to an anisotropy field that starts to play a more important role around the compensation point where the dipolar interactions are small. The relative abundance and distribution of these two different magnetic domains then determines the SMR response, as also

modelled in more detail in the supplemental materials. While this explanation is simple and plausible, a more in-depth comparison between experiment and model would require spatially resolved imaging of the sublattice domain orientations around T_{comp} in order to understand the evolution of the SMR with temperature. However this is beyond the scope of the current work that is based on transport measurements.

To elucidate the multi-maxima response further, we carry out SMR measurements for different magnetic field amplitudes and find that the signal depends on the magnetic field strength: Figure 4(a)-(d) show the angular dependent SMR for magnetic fields of $|\mu_0 \boldsymbol{H}|$ = 0.8 T, 3 T, 5 T and 7 T at a fixed temperature 182 K, respectively. When increasing the field, the shape of the SMR changes significantly: For $|\mu_0 \boldsymbol{H}|$ = 0.8 T, only two maxima are observed and the angular dependence deviates significantly from the $\sin^2\beta$ relation. Interestingly, when the field is further increased to 3 T, the SMR shows the main maxima around $\beta = 180°$ and $360°$ and small maxima near $\beta = 90°$ and $270°$. At $|\mu_0 \boldsymbol{H}|$ = 5 T, the SMR maxima around $\beta = 90°$ and $270°$ are comparable to the maxima around $\beta = 180°$ and $360°$. Eventually, at $|\mu_0 \boldsymbol{H}|$ = 7 T two maxima around $\beta = 90°$ and $270°$ dominate. The relative strength of the two maxima at $\beta = 90°$ and $180°$, which we interpret here in terms of the relative contribution from collinear and non-collinear domains, depends strongly on the magnitude of fields, which is similar to the influence of the temperature on the magnetization configurations as discussed in Fig. 3, indicating a field-induced transformation of multi-domain states in the GdIG sample. In particular, the temperature where the minimum SMR amplitude is observed increases with increasing magnetic field. Our SMR results are consistent with the field induced reorientation of magnetic sublattices revealed by element-specific x-ray magnetic circular dichroism (XMCD) measurements [33,40], showing that we can switch between the different regimes by either varying the temperature or the applied magnetic field. This effect might indicate that the sublattice configuration in the GdIG thin film is more complex than in the bulk, or that the moments close to the magnet/metal interface show more complex physics. To quantify this issue, however, more detailed work will be needed in the future.

4. Conclusion

In conclusion, we have systematically measured the temperature and field dependent SMR in GdIG/Pt bilayers around the compensation temperature of GdIG. The temperature dependence and amplitude of the SMR within the collinear regime of GdIG are quantitatively consistent with those observed for YIG, which suggests that the Gd magnetic sublattice plays a minor role for the SMR response as compare to the Fe sublattices. Due to the non-collinear magnetic structure close to T_{comp}, the angular dependent SMR signal deviates significantly from the usual $\sin^2\theta$ relation. Both an inverted SMR signal, and a multi-maxima response with relative strengths depending strongly on temperature and field strength are observed. The complex dependence of SMR behavior

on temperature and magnetic field magnitude can be qualitatively described by the co-existence of collinear and canted domain states that are distributed on the length scale probed in the sample around the compensation temperature, which is directly reflected in the number and strength of the maxima in the SMR signal. By varying the applied field, we demonstrate that we can switch between collinear and non-collinear regimes showing that the observed effect can be used as an alternative approach for identifying the magnetization state in non-collinear ferrimagnets by SMR measurements.

Note added. During the preparation of this manuscript, Vélez *et al.*[34] and Hou *et al*.[41] have reported the inverted SMR in surface treated YIG/Pt and YIG/NiO/Pt systems, and they attribute their results to the magnetic frustration of YIG at low temperature and the spin-flop coupling between NiO and YIG, respectively. Both their results and ours show high sensitivity of SMR on the magnetization configuration of FMI at the interface.

Acknowledgments

The authors would like to express their thanks to Prof. Dr. Kathrin Dörr at Martin-Luther-Universität Halle-Wittenberg for help with the sample preparation. This work was supported by Deutsche Forschungsgemeinschaft (DFG) SPP 1538 “Spin Caloric Transport” (project GO 944/4), the Graduate School of Excellence Materials Science in Mainz (MAINZ), the EU projects (IFOX, NMP3-LA-2012246102, INSPIN FP7-ICT-2013-X 612759, MASPIC ERC-2007-StG 208162), DAAD Spintronics networks (SpinNet, MaHoJeRo), projects No. 56268455, 57334897 and the Transregional Collaborative Research Center (SFB/TRR) 173 “Spin+X – Spin its collective environment”.

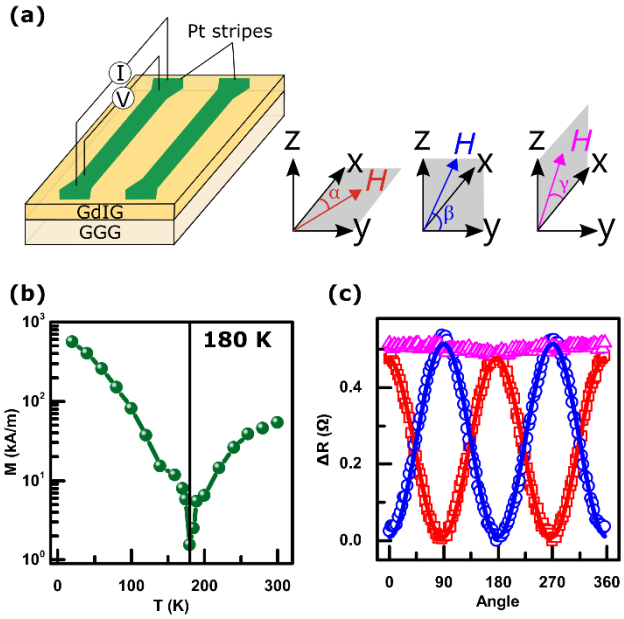

FIG. 1. (a) Sketch of the sample GGG/GdIG/Pt and measurement schematics. (b) Magnetization of the sample as a function of temperature at $|\mu_0 \boldsymbol{H}|$ = 0.1 T. The compensation temperature is around 180 K. The data was taken from ref.[16], ACS. (c) ADMR signal measured at 295 K when rotating a magnetic field $|\mu_0 \boldsymbol{H}|$ = 0.8 T in xy (red), yz (blue) and xz (pink) planes, respectively.

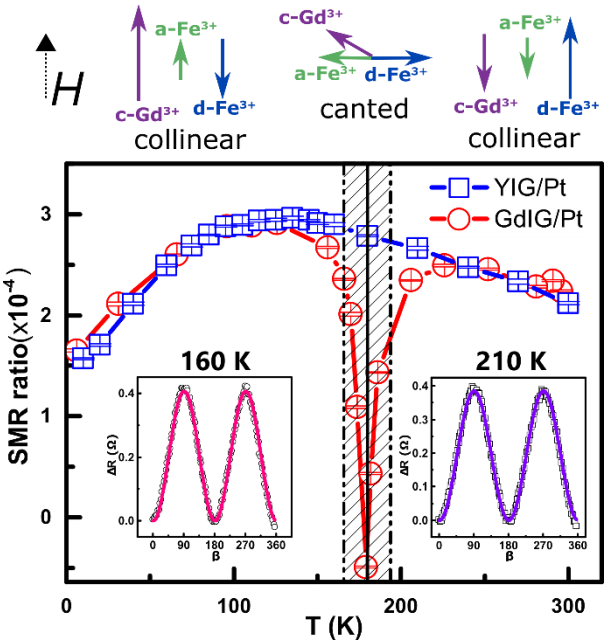

FIG. 2. SMR ratio at $|\mu_0 \boldsymbol{H}|$ = 0.8 T as a function of temperature for GdIG/Pt (open red circles) and YIG/Pt (open blue squares), respectively. The solid line is a guide to the eye. The shaded area indicates the temperature range close to the compensation temperature, where a magnetic canting phase in expected. The left and right insets depict the SMR measured at temperatures far above and far below the compensation temperature, respectively. Upper panel: Sketch of magnetization orientations of the three sublattices far above, around and far below the compensation temperature, respectively.[33]

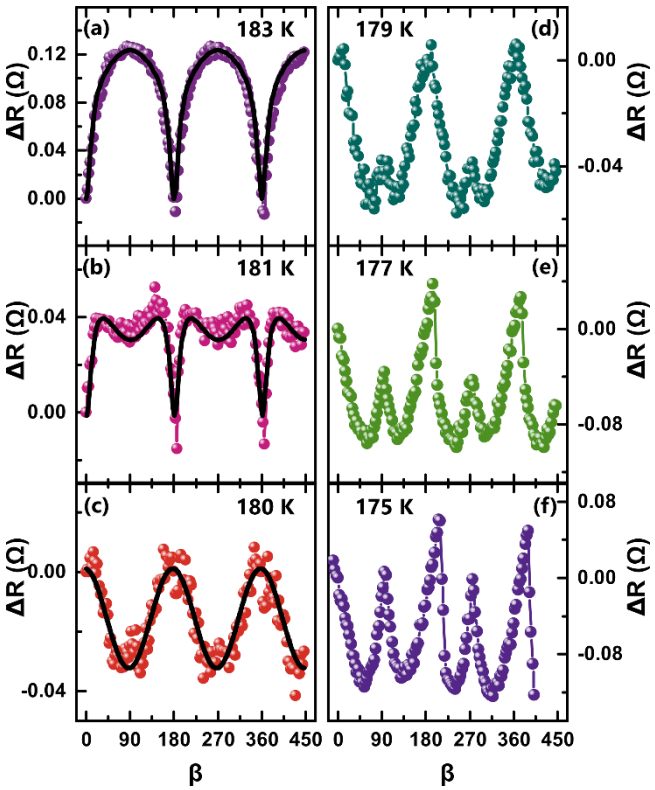

FIG. 3. (a)-(f) SMR signal as a function of magnetic field angle at temperatures T = 183 K, 181 K, 180 K, 179 K, 177 K and 175 K, respectively. The solid lines shown at 183 K and 181 K are simulated using the method described in the supplementary materials. The error of the temperature is less than 20 mK. The applied field is 0.8 T.

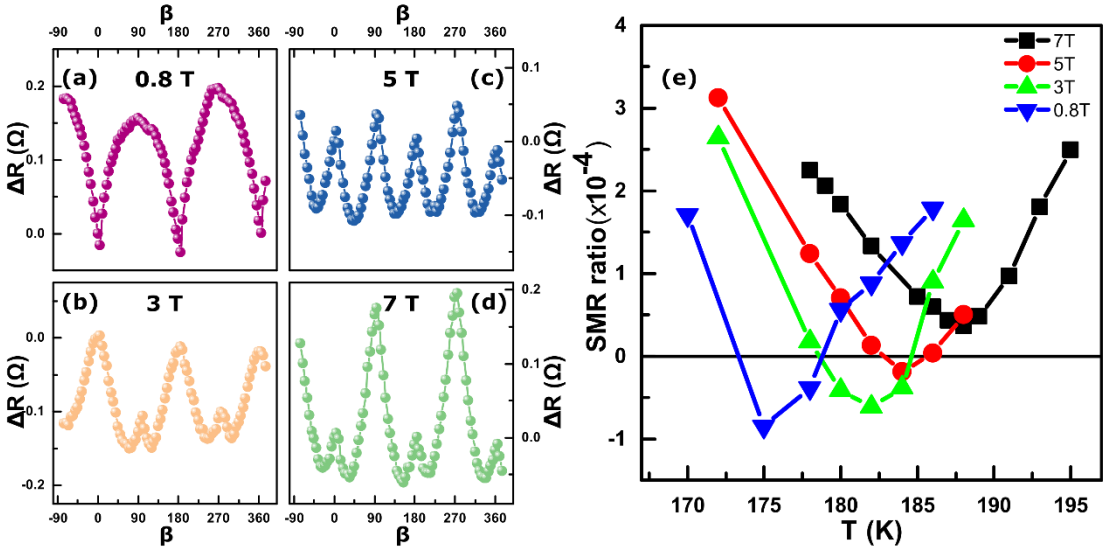

FIG. 4. (a)-(d) SMR signal as a function of the magnetic field orientation for $|\mu_0 \boldsymbol{H}|$ = 0.8 T, 3 T, 5 T and 7 T, respectively. The temperature is fixed at 182 K. (e) SMR ratio as a function of temperature for GdIG/Pt with different external field $|\mu_0 \boldsymbol{H}|$ = 0.8 T (blue), 3 T (green), 5 T (red) and 7 T (black), respectively. Note that the temperatures shown here are slightly different from the ones used in the other measurements as they were obtained in a different measurement set-up where the position of the temperature sensors leads to a slightly different read out value.

References

[1] I. Žutić, J. Fabian, and S. Das Sarma 2004 *Rev. Mod. Phys.* **76** 323

[2] S. Maekawa, S. O. Valenzuela, E. Saitoh, and A. Kimura 2012 *Spin current* (Oxford: Oxford University Press)

[3] Y. Tserkovnyak, A. Brataas, and G. E. W. Bauer 2002 *Phys. Rev. Lett.* **88** 117601

[4] Y. Tserkovnyak, A. Brataas, and G. E. W. Bauer 2002 *Phys. Rev. B* **66** 224403

[5] F. D. Czeschka, L. Dreher, M. S. Brandt, M. Weiler, M. Althammer, I. M. Imort, G. Reiss, A. Thomas, W. Schoch, W. Limmer, H. Huebl, R. Gross, and S. T. B. Goennenwein 2011 *Phys. Rev. Lett.* **107** 046601

[6] Y. Tserkovnyak, A. Brataas, G. E. W. Bauer, and B. I. Halperin 2005 *Rev. Mod. Phys.* **77** 1375

[7] K. Uchida, J. Xiao, H. Adachi, J. Ohe, S. Takahashi, J. Ieda, T. Ota, Y. Kajiwara, H. Umezawa, H. Kawai, G. E. W. Bauer, S. Maekawa, and E. Saitoh 2010 *Nat. Mater.* **9** 894

[8] C. M. Jaworski, J. Yang, S. Mack, D. D. Awschalom, J. P. Heremans, and R. C. Myers 2010 *Nat. Mater.* **9** 898

[9] M. Weiler, M. Althammer, F. D. Czeschka, H. Huebl, M. S. Wagner, M. Opel, I.-M. Imort, G. Reiss, A. Thomas, R. Gross, and S. T. B. Goennenwein 2012 *Phys. Rev. Lett.* **108** 106602

[10] G. E. W. Bauer, E. Saitoh, and B. J. van Wees 2012 *Nat. Mater.* **11** 391

[11] D. Qu, S. Y. Huang, J. Hu, R. Wu, and C. L. Chien 2013 *Phys. Rev. Lett.* **110**

[12] N. Roschewsky, M. Schreier, A. Kamra, F. Schade, K. Ganzhorn, S. Meyer, H. Huebl, S. Geprägs, R. Gross, and S. T. B. Goennenwein 2014 *Appl. Phys. Lett.* **104** 202410

[13] A. Kehlberger, U. Ritzmann, D. Hinzke, E.-J. Guo, J. Cramer, G. Jakob, M. C. Onbasli, D. H. Kim, C. A. Ross, M. B. Jungfleisch, B. Hillebrands, U. Nowak, and M. Kläui 2015 *Phys. Rev. Lett.* **115** 096602

[14] S. Geprägs, A. Kehlberger, F. D. Coletta, Z. Qiu, E.-J. Guo, T. Schulz, C. Mix, S. Meyer, A. Kamra, M. Althammer, H. Huebl, G. Jakob, Y. Ohnuma, H. Adachi, J. Barker, S. Maekawa, G. E. W. Bauer, E. Saitoh, R. Gross, S. T. B. Goennenwein, and M. Kläui 2016 *Nat. Commun.* **7** 10452

[15] Y. H. Shen, X. S. Wang, and X. R. Wang 2016 *Phys. Rev. B* **94** 014403

[16] J. Cramer, E.-J. Guo, S. Geprägs, A. Kehlberger, Y. P. Ivanov, K. Ganzhorn, F. Della Coletta, M. Althammer, H. Huebl, R. Gross, J. Kosel, M. Kläui, and S. T. B. Goennenwein 2017 *Nano Lett.* **17** 3334

[17] J. E. Hirsch 1999 *Phys. Rev. Lett.* **83** 1834

[18] S. Zhang 2000 *Phys. Rev. Lett.* **85** 393

[19] J. Sinova, S. O. Valenzuela, J. Wunderlich, C. H. Back, and T. Jungwirth 2015 *Rev. Mod. Phys.* **87** 1213

[20] E. Saitoh, M. Ueda, H. Miyajima, and G. Tatara 2006 *Appl. Phys. Lett.* **88** 182509

[21] K. Ando, Y. Kajiwara, K. Sasage, K. Uchida, and E. Saitoh 2010 *IEEE Trans. Magn.* **46** 3694

[22] X. Jia, K. Liu, K. Xia, and G. E. W. Bauer 2011 *Europhys. Lett.* **96** 17005

[23] H. Nakayama, M. Althammer, Y.-T. Chen, K. Uchida, Y. Kajiwara, D. Kikuchi, T. Ohtani, S. Geprägs, M. Opel, S. Takahashi, R. Gross, G. E. W. Bauer, S. T. B. Goennenwein, and E. Saitoh 2013 *Phys. Rev. Lett.* **110** 206601

[24] Y.-T. Chen, S. Takahashi, H. Nakayama, M. Althammer, S. T. B. Goennenwein, E. Saitoh, and G. E. W. Bauer 2013 *Phys. Rev. B* **87** 144411

[25] Y.-T. Chen, S. Takahashi, H. Nakayama, M. Althammer, S. T. B. Goennenwein, E. Saitoh, and G. E. W. Bauer 2016 *J. Phys.: Condens. Matter* **28** 103004

[26] N. Vlietstra, J. Shan, V. Castel, B. J. van Wees, and J. Ben Youssef 2013 *Phys. Rev. B* **87** 184421

[27] S. Meyer, M. Althammer, S. Geprägs, M. Opel, R. Gross, and S. T. B. Goennenwein 2014 *Appl. Phys. Lett.* **104** 242411

[28] M. Althammer, S. Meyer, H. Nakayama, M. Schreier, S. Altmannshofer, M. Weiler, H. Huebl, S. Geprägs, M. Opel, R. Gross, D. Meier, C. Klewe, T. Kuschel, J.-M. Schmalhorst, G. Reiss, L. Shen, A. Gupta, Y.-T. Chen, G. E. W. Bauer, E. Saitoh, and S. T. B. Goennenwein 2013 *Phys. Rev. B* **87** 224401

[29] Z. Ding, B. L. Chen, J. H. Liang, J. Zhu, J. X. Li, and Y. Z. Wu 2014 *Phys. Rev. B* **90** 134424

[30] S. R. Marmion, M. Ali, M. McLaren, D. A. Williams, and B. J. Hickey 2014 *Phys. Rev. B* **89** 220404
[31] M. Aldosary, J. Li, C. Tang, Y. Xu, J.-G. Zheng, K. N. Bozhilov, and J. Shi 2016 *Appl. Phys. Lett.* **108** 242401
[32] A. Aqeel, N. Vlietstra, J. A. Heuver, G. E. W. Bauer, B. Noheda, B. J. van Wees, and T. T. M. Palstra 2015 *Phys. Rev. B* **92** 224410
[33] K. Ganzhorn, J. Barker, R. Schlitz, B. A. Piot, K. Ollefs, F. Guillou, F. Wilhelm, A. Rogalev, M. Opel, M. Althammer, S. Geprägs, H. Huebl, R. Gross, G. E. W. Bauer, and S. T. B. Goennenwein 2016 *Phys. Rev. B* **94** 094401
[34] A. Aqeel, N. Vlietstra, A. Roy, M. Mostovoy, B. J. van Wees, and T. T. M. Palstra 2016 *Phys. Rev. B* **94** 134418
[35] R. Metselaar and P. K. Larsen 1974 *Solid State Commun.* **15** 291
[36] G. F. Dionne 2009 *Magnetic Oxides* (New York: Springer)
[37] R. Pauthenet 1958 *J. Appl. Phys.* **29** 253
[38] E. Sawatzky and E. Kay 1969 *J. Appl. Phys.* **40** 1460
[39] T. Lin, C. Tang, H. M. Alyahayaei, and J. Shi 2014 *Phys. Rev. Lett.* **113** 037203
[40] C. Strohm, T. Roth, C. Detlefs, P. van der Linden, and O. Mathon 2012 *Phys. Rev. B* **86** 214421
[41] D. Hou, Z. Qiu, J. Barker, K. Sato, K. Yamamoto, S. Vélez, J. M. Gomez-Perez, L. E. Hueso, F. Casanova, and E. Saitoh 2017 *Phys. Rev. Lett.* **118** 147202